

We are IntechOpen, the world's leading publisher of Open Access books Built by scientists, for scientists

6,900

Open access books available

186,000

International authors and editors

200M

Downloads

Our authors are among the

154

Countries delivered to

TOP 1%

most cited scientists

12.2%

Contributors from top 500 universities



WEB OF SCIENCE™

Selection of our books indexed in the Book Citation Index
in Web of Science™ Core Collection (BKCI)

Interested in publishing with us?
Contact book.department@intechopen.com

Numbers displayed above are based on latest data collected.
For more information visit www.intechopen.com



Classifiers of Digital Modulation Based on the Algorithm of Fast Walsh-Hadamard Transform and Karhunen-Loeve Transform

Richterova Marie and Mazalek Antonin
*University of Defence
Czech Republic*

1. Introduction

Automatic recognition of modulation is rapidly evolving area of signal analysis. In recent years, much interest by academic and military research institutes has focused around the research and development of recognition algorithms modulation. There are two main reasons to know the correct modulation type of a signal: to preserve the signal information content and to decide the suitable counter action such as jamming (Nandi & Azzouz, 1998), (Grimaldi et al, 2007), (Park & Dae, 2006).

From this viewpoint, considerable attention is being paid to the research and development of algorithms for the recognition of modulated signals. The need of practice made it necessary to solve the questions of automatic classification of samples of received signals with use of computers and available software.

In this chapter, a new original configuration of subsystems for the automatic modulation recognition of digital signals is described. The signal recognizer being developed consists of five subsystems: (1) adaptive antenna arrays, (2) pre-processing of signals, (3) key features extraction, (4) modulation recognizer and (5) output stage.

This chapter describes the use of Walsh-Hadamard transform (WHT) and Karhunen-Loeve transform (KLT) for the modulation recognition in high frequency (HF) and very high frequency (VHF) bands. The input real signal is pre-processed and converted to the "phase image". The WHT and KLT is applied and the dimensionality reduction is implemented and the classifier recognized the signal. The clustering analysis method was chosen by acclamation for 2-class and 3-class recognition of 2-FSK, 4-FSK and PSK signals. The 2-class and 3-class minimum-distance modulation classifier was created in the MATLAB programme. The tests of designed algorithm were implemented on real signal patterns.

2. Orthogonal transforms used for modulation recognition

The utilization of orthogonal transforms for the recognition of various types of modulated signals is described in a number of reference sources. Fourier transform (Ahmed & Rao, 1975), (Jondral, 1991), Haar transform (Ahmed & Rao, 1975), discrete cosine transform (Ahmed & Rao, 1975), (Jondral, 1991), Walsh-Hadamard transform (WHT) (Ahmed & Rao, 1975), (Richterova, 1997, 2001) and Karhunen-Loeve transform (KLT) (Hua & Liu, 1998),

(Richterova, 2001), (Richterova & Juracek, 2006) belong to the most frequently exploited and recommended orthogonal transforms. In this chapter, the use of WHT and KLT for the recognition of the frequency shift keying (2-FSK and 4-FSK) signals and the phase shift keying (2-PSK and 4-PSK) signals will be described.

2.1 Walsh-Hadamard transform

The Walsh-Hadamard transform (WHT) is perhaps the most well-known of the nonsinusoidal orthogonal transforms. The WHT has gained prominence in various digital signal processing applications, since it can essentially be computed using additions and subtractions only. WHT is used for the Walsh representation of the data sequences. Their basis functions are sampled Walsh functions which can be expressed in terms of the Hadamard matrix. The WHT is defined by relation (Ahmed & Rao, 1975),

$$B(N) = \frac{1}{N} H(N) \cdot X(N), \quad (1)$$

where :

$B(N)$ - coefficients of WHT,

N - order of the WHT,

$H(N)$ - N -order Hadamard matrix,

$X(N)$ - signal vector.

An algorithm for the WHT was realized in the MATLAB programme.

2.2 Karhunen-Loeve transform

The Karhunen-Loeve transform (Hua & Liu, 1998) (named after Kari Karhunen and Michel Loeve) is a representation of a stochastic process as an infinite linear combination of orthogonal functions, analogous to a Fourier series representation of a function on a bounded interval.

In contrast to a Fourier series, where the coefficients are real numbers and the expansion basis consists of sinusoidal functions (that is, sine and cosine functions), the coefficients in the Karhunen-Loeve transform are random variables and the expansion basis depends on the process. In fact, the orthogonal basis functions used in this representation are determined by the covariance function of the process. The KLT is a key element of many signal processing and communication tasks.

The Karhunen-Loeve Transform (KLT), also known as Hotelling Transform and Eigenvector Transform, is closely related to the Principal Component Analysis (PCA) and widely used in many fields of data analysis.

Let Φ_k be the eigenvector corresponding to the k th eigenvalue λ_k of the covariance matrix \sum_x , i.e.,

$$\sum_x \Phi_k = \lambda_k \Phi_k \quad (k = 0, \dots, N-1) \quad (2)$$

or in matrix form:

$$\begin{bmatrix} \dots & \dots & \dots \\ \dots & \sigma_{ij} & \dots \\ \dots & \dots & \dots \end{bmatrix} \begin{bmatrix} \Phi_k \end{bmatrix} = \lambda_k \begin{bmatrix} \Phi_k \end{bmatrix} \quad (k = 0, \dots, N-1) \quad (3)$$

As the covariance matrix $\sum_x = \sum_x^T$ is symmetric (Hermitian if \bar{x} is complex), its eigenvectors Φ_i are orthogonal:

$$(\Phi_i, \Phi_j) = \Phi_i^T \Phi_j = \begin{cases} 1 & i = j \\ 0 & i \neq j \end{cases} \quad (4)$$

and we can construct an $N \times N$ orthogonal (unitary) matrix Φ

$$\Phi \cong [\Phi_0, \dots, \Phi_{N-1}] \quad (5)$$

satisfying

$$\Phi^T \Phi = I, \text{ i.e., } \Phi^{-1} = \Phi^T \quad (6)$$

The N eigenequations above can be combined to be expressed as:

$$\sum_x \Phi = \Phi \Lambda \quad (7)$$

or in matrix form:

$$\begin{bmatrix} \dots & \dots & \dots \\ \dots & \sigma_{ij} & \dots \\ \dots & \dots & \dots \end{bmatrix} [\Phi_0, \dots, \Phi_{N-1}] = [\Phi_0, \dots, \Phi_{N-1}] \begin{bmatrix} \lambda_0 & 0 & \dots & 0 \\ 0 & \lambda_1 & 0 & \vdots \\ \vdots & 0 & \ddots & 0 \\ 0 & \dots & 0 & \lambda_{N-1} \end{bmatrix} \quad (8)$$

Here Λ is a diagonal matrix $\Lambda = \text{diag}(\lambda_0, \dots, \lambda_{N-1})$. Left multiplying $\Phi^T = \Phi^{-1}$ on both sides, the covariance matrix \sum_x can be diagonalized:

$$\Phi^T \sum_x \Phi = \Phi^{-1} \sum_x \Phi = \Phi^{-1} \Phi \Lambda = \Lambda \quad (9)$$

Now, given a signal vector \bar{x} , we can define the orthogonal (unitary if \bar{x} is complex) Karhunen-Loeve Transform of \bar{x} as:

$$y = \begin{bmatrix} y_0 \\ y_1 \\ \vdots \\ y_{N-1} \end{bmatrix} = \Phi^T x = \begin{bmatrix} \Phi_0^T \\ \Phi_1^T \\ \vdots \\ \Phi_{N-1}^T \end{bmatrix} x \quad (10)$$

where the i th component y_i of the transform vector is the projection of \bar{x} onto Φ_i :

$$y_i = (\Phi_i, x) = \Phi_i^T x \quad (11)$$

Left multiplying $\Phi = (\Phi^T)^{-1}$ on both sides of the transform $y = \Phi^T x$, we get the inverse transform:

$$x = \Phi y = [\Phi_0, \Phi_1, \dots, \Phi_{N-1}] \begin{bmatrix} y_0 \\ y_1 \\ \vdots \\ y_{N-1} \end{bmatrix} = \sum_{i=0}^{N-1} y_i \Phi_i \quad (12)$$

By this transform we see that the signal vector \bar{x} is now expressed in an N-dimensional space spanned by the N eigenvectors Φ_i ($i=0, \dots, N-1$) as the basis vectors of the space. An algorithm for the KLT was realized in the MATLAB programme.

3. Principle of the recognition of FSK and PSK signals

The common fundamental diagram for recognition of 2-FSK, 4-FSK and PSK signals is introduced in Fig. 1 (Richterova, 1999, 2001). General principle of this system for recognition will be described in next text.

The inquiry analog signal $x(t)$ enters into an A/D converter, where it subjects sampling, quantization and make-up into matrix 32x32. This way, we obtain a "phase image" of the inquiry input signal $x(t)$. The orthogonal transform (KLT or WHT) is implemented on this matrix of "phase image" with the aim to emphasize important elements image and at the same time to suppress the circumstantial and disturbing elements and the components.

The property of Karhunen-Loeve transform will be used for the recognition of 2-FSK, 4-FSK and PSK signals. All samples of signal pattern are not needed to the proper recognition; it is possible to use the dimensional reduction of the matrix. The proper classification of signal and his enlistment into corresponding group of signals follow up the block of orthogonal transform.

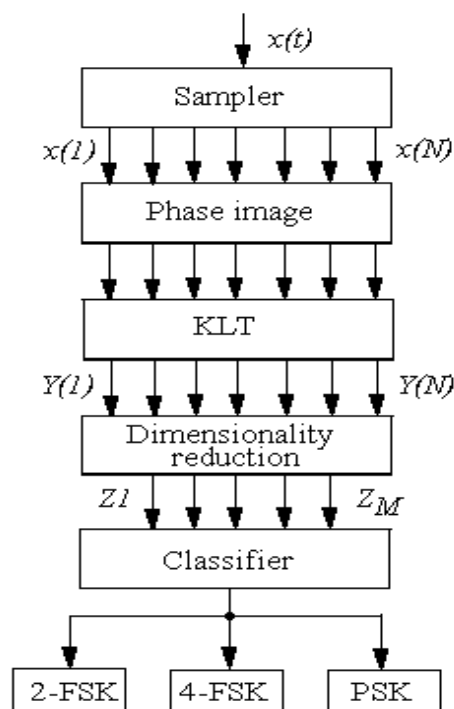


Fig. 1. Block diagram for recognition of digital modulated signals

The minimum distance classifier will be used for the solution of the problem of the recognition of 2-FSK, 4-FSK and PSK signals. The principle of minimum distance classifier will be described in the next section.

3.1 Phase image

The input signal is given by sequence of the samples corresponding to the digital form of recognition signal. The input vector has the length of 2048 samples. The "phase image" of modulated signal is composed so, that they are generated of points about "the coordinates" - the value of sample and the difference between samples.

These points are mapping into the rectangular net about proportions 32 x 32 so, that a relevant point of net is allocated the number one. If more points fall through into the identical node, then is adding the number one next. These output values are standardized and quantized (Richterova, 1997, 1999, 2001), (Richterova & Juracek, 2006). The "phase images" of 2-FSK and 4-FSK signals are presented on Fig. 2.

Lower frequency of FSK signal corresponds to the ellipse, which lies near to centre of image. Higher frequency of FSK signal corresponds to the ellipse, which is on the margin of image. The "phase image" of PSK is one ellipse.

3.2 The 3-class minimum-distance classifier

The minimum-distance classifier is designed to operate on the following decision rule (Ahmed & Rao, 1975), (Richterova, 2001), (Richterova & Juracek, 2006):

A given pattern Z belongs to C_i , if Z is closest to $\bar{Z}_i, i=1,2,3 \dots$

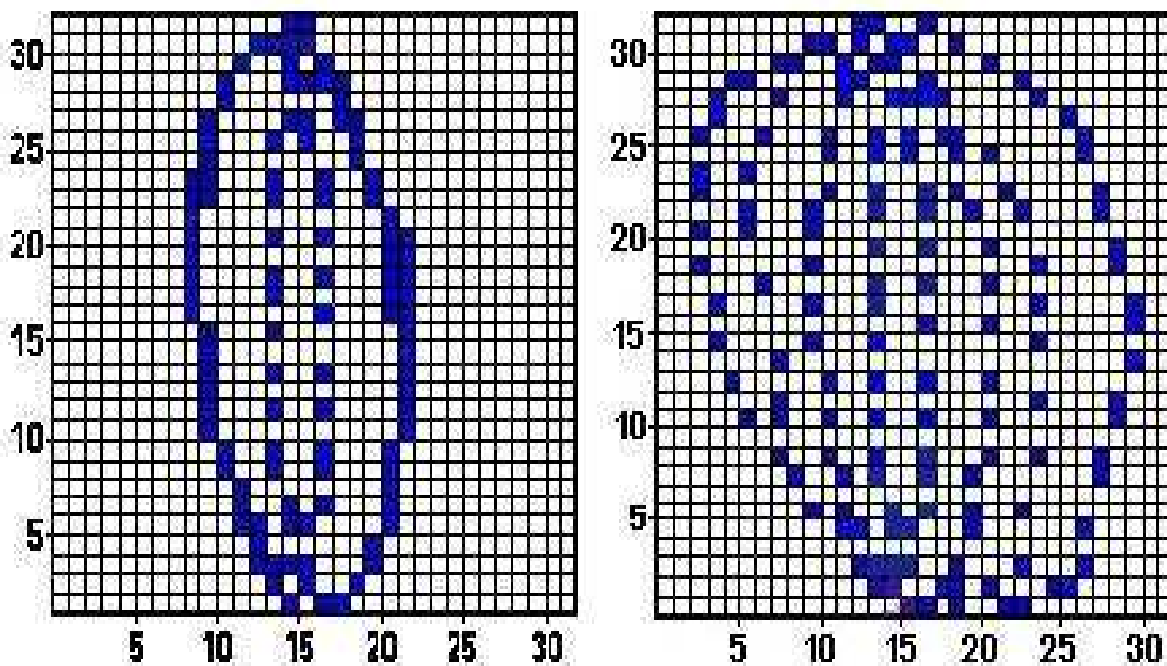


Fig. 2. "Phase images" of 2-FSK signal and "phase image" of 4-FSK signal

Let D_i denote the distance of Z from $\bar{Z}_i, i=1,2,3$. Then we have [see Fig 3]

$$D_i^2 = \|Z - \bar{Z}_i\|^2 = (Z - \bar{Z}_i)' (Z - \bar{Z}_i), \quad (13)$$

Simplification of D_i yields

$$D_i^2 = \|Z\|^2 - 2 \cdot \left(\bar{Z}_i Z - \frac{1}{2} \|\bar{Z}_i\|^2 \right), \quad (14)$$

Clearly, D_i^2 is a minimum, when the quantity $\left(\bar{Z}_i Z - \frac{1}{2} \|\bar{Z}_i\|^2 \right)$ is a maximum. Thus, rather than having the classifier compute D_i^2 in Eq. (13), it is simpler to require it to compute the quantity $\left(\bar{Z}_i Z - \frac{1}{2} \|\bar{Z}_i\|^2 \right)$. The classifier is then described by the discriminant functions

$$g_i(Z) = \bar{Z}_i Z - \frac{1}{2} \|\bar{Z}_i\|^2, \quad i=1,2,3 \quad (15)$$

The classifier thus computes three numbers $g_1(Z)$, $g_2(Z)$, $g_3(Z)$ as shown in Fig. 3 and then compares them. It assigns Z to C_1 if $g_1(Z)$ is maximum, to C_2 if $g_2(Z)$ is maximum and to C_3 if $g_3(Z)$ is maximum.

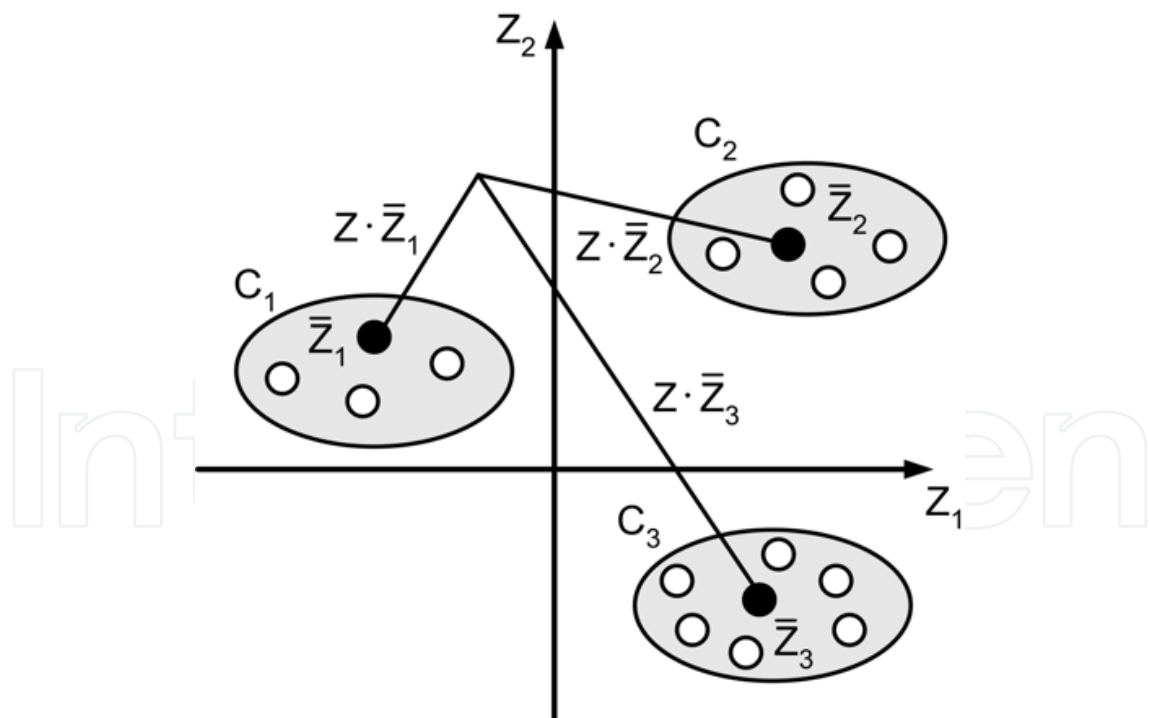


Fig. 3. 3-class classifier of FSK and PSK signals

3.3 The 2-class minimum-distance classifier

The process of the recognition of 2-FSK and 4-FSK signals by means of the 2-class minimum distance classifier is shown in Fig.4.

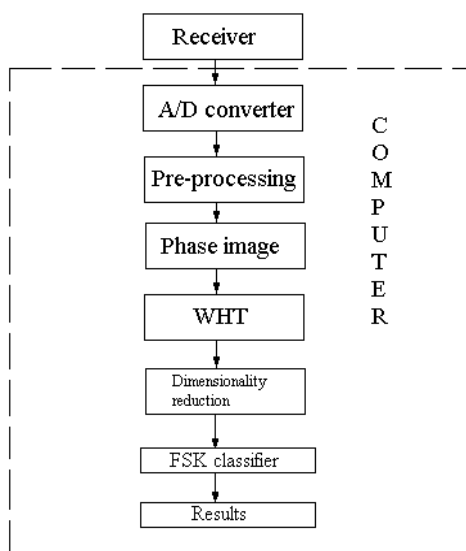


Fig. 4. Simplified block scheme of a recogniser of 2-FSK and 4-FSK signals

Now we briefly describe the block scheme from Fig. 4. A real signal inputs from a receiver via an A/D converter into a computer, where it is processed and stored in the data format WAV. Then block is pre-processed and used for the filtering and scaling of the input vector of real pattern of 2-FSK or 4-FSK signal. The scaling of real pattern signal is performed in this case and the spectral power density signal is calculated by means of the function PSD, which is implemented in the MATLAB programme. By testing of PSD waveform is processed the classification in to FSK or PSK signals.

The phase image (Fig. 2) of the processed pattern of real signal is created by means of algorithms described in (Richterova, 1997, 2001).

The feature vector is a result of the pre-processing of the real signal pattern. The feature vector is classified via a minimum-distance classifier.

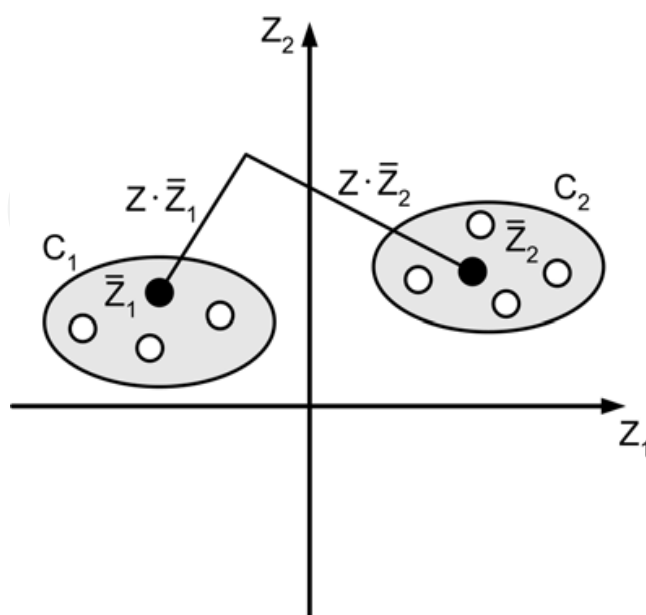


Fig. 5. A 2-class classifier of FSK or PSK signals

Two 2-class minimum-distance classifiers for 2-FSK and 4-FSK signals and two 2-class minimum-distance classifiers for 2-PSK and 4-PSK signals were designed and realized via the learning process. The learning process and the working principle of these minimum-distance classifiers are described in (Ahmed & Rao, 1975), (Richterova, 1997, 2001). The practical application of 2-class minimum-distance classifiers is presented in (Richterova, 1997, 2001).

4. Experimental results for 2-class classifier

The performance evaluations of the proposed 2-class minimum-distance classifier (see Fig.4) are introduced for 2-FSK and 4-FSK signals and for 2-PSK and 4-PSK. We have classified 42 real patterns of FSK signals. Parameters of real FSK signal patterns, which were used to experimental process, are presented in Table 1.

Modulation type	Carrier frequency [Hz]	Sampling frequency [Hz]	Modulation velocity [Bd]
2-FSK	2400	44100	150
4-FSK	4800	44100	150
2-FSK	4800	44100	100
4-FSK	2400	44100	100
2-FSK	1200	44100	50
4-FSK	4800	44100	200

Table 1. Parameters of real 2-FSK and 4-FSK patterns

We have classified 32 real patterns of PSK signals. Parameters of real PSK signal patterns, which were used to experimental process, are presented in Table 2.

Modulation type	Carrier frequency [Hz]	Sampling frequency [Hz]	Modulation velocity [Bd]
2-PSK	2400	44100	150
4-PSK	4800	44100	150
2-PSK	4800	44100	100
4-PSK	2400	44100	100
2-PSK	4800	44100	200
4-PSK	4800	44100	200

Table 2. Parameters of real 2-PSK and 4-PSK patterns

The results of the performance are summarized in Table 3 for the classifier based on the WHT and FSK signals.

Real pattern signals	Classified modulation type [%]	
	2-FSK	4-FSK
2-FSK	87,0	13,0
4-FSK	15,0	85,0

Table 3. Performance of the 2-class minimum-distance classifier of FSK based on the WHT

The results of the performance are presented in Table 4 for the classifier based on the WHT and PSK signals.

Real pattern signals	Classified modulation type [%]	
	2-PSK	4-PSK
2-FSK	77,0	23,0
4-FSK	25,0	75,0

Table 4. Performance of the 2-class minimum-distance classifier of PSK signals based on the WHT

The results of the performance are summarized in Table 5 for the classifier based on the KLT and FSK signals.

Real pattern signals	Classified modulation type [%]	
	2-FSK	4-FSK
2-FSK	87,0	13,0
4-FSK	15,0	85,0

Table 5. Performance of the 2-class minimum-distance classifier of FSK based on the KLT

The results of the performance are presented in Table 6 for the classifier based on the KLT and PSK signals.

Real pattern signals	Classified modulation type [%]	
	2-PSK	4-PSK
2-FSK	77,0	23,0
4-FSK	25,0	75,0

Table 6. Performance of the 2-class minimum-distance classifier of PSK signals based on the KLT

5. Experimental results for a 3-class classifier

The learning process of the 3-class minimum-distance classifier was effected for 30 realizations of the simulation patterns of 2-FSK, 4-FSK, 2-PSK and 4-PSK signals with the modulation velocity 50, 100, 150 and 200 Bd and SNR 15, 20, 30 [dB].

The experimental tests for the 3-class minimum-distance classifier were implemented on 200 realizations of real patterns of 2-FSK, 4-FSK, 2-PSK and 4-PSK signals. Parameters of real signal patterns, which were used to experimental process, are presented in Table 7.

The results of classification of modulation type for 200 realizations of 2-FSK, 4-FSK, 2-PSK and 4-PSK signals are introduced in Table 8.

Modulation type	Carrier frequency [Hz]	Sampling frequency [Hz]	Modulation velocity [Bd]
2-FSK	2400	44100	150
4-FSK	4800	44100	150
2-PSK	2400	44100	100
4-PSK	2400	44100	100

Table 7. Parameters of real digital modulation patterns

Modulation type	Correct classification in [%] for KLT	Correct classification in [%] for WHT
2-FSK	75	78
4-FSK	72	76
PSK	64	62

Table 8. Results of classification of modulation type by 3-class minimum-distance classifier for 200 realizations

The results of classification of PSK signal show, that the classifier based on orthogonal transform have not optimal solution for problems of classification of real PSK signals. We are explored other solution of classification of PSK signals. We want to introduce simple classifier of PSK signal based on cyclostationary feature detection.

This next section introduced the basic cyclostationary descriptors and on simply experiments demonstrates the effectiveness of this approach and its resistance against additive white Gaussian noise (AWGN). The high resistance level results from correlation principle of cyclostationary method because mean value of correlation of AWGN signal is zero.

There are many important aspects in cyclostationary measurement and application; one of them is high sensitivity of obtained results on input parameters that is to say the input sequence length and required cyclic and frequency resolution. In some applications, the input signal pre-processing is necessary. The future research will be focused on automatic modulation recognition.

6. Cyclostationary signals descriptors

A random process $x(t)$ is said to be N th order cyclostationary in the strict sense if its N th order distribution function exhibits periodicity in time with period T (Gardner et al., 2006)

$$F(x_1, x_2, \dots, x_n; t_1, t_2, \dots, t_n) = F(x_1, x_2, \dots, x_n; t_1 + mT, t_2 + mT, \dots, t_n + mT) \quad (16)$$

In practice it is often sufficient to use only second order statistics which leads to the definition of second-order cyclostationarity in wide sense. The key second order statistical characteristic is instantaneous autocorrelation function $R_{xx}(t, \tau)$. So, the process $x(t)$ is said to be cyclostationary in a wide sense if its autocorrelation function is periodic in time with period T

$$R_{xx}(t, \tau) = R_{xx}(t + mT, \tau) \quad (17)$$

where the instantaneous autocorrelation function is defined as (Semmlow, 2004)

$$R_{xx}(t, \tau) = x(t + \tau/2)x^*(t - \tau/2) \quad (18)$$

where τ is the time lag and $*$ represents the complex conjugate of the signal $x(t)$. Because the instantaneous autocorrelation function is periodic in time (for all τ) it can be expanded as Fourier series

$$R_{xx}(t, \tau) = \sum_{n=-\infty}^{+\infty} R_{xx}^{\alpha}(\tau) e^{i2\pi n t} \quad (19)$$

where $\alpha = n / T$ are called cyclic frequencies, and $R_{xx}^\alpha(\tau)$ are the Fourier coefficients of the instantaneous autocorrelation function that are also referred to as cyclic autocorrelation function

$$R_{xx}^\alpha(\tau) = \frac{1}{T} \int_{-\frac{T}{2}}^{\frac{T}{2}} R_{xx}(t, \tau) e^{-i2\pi\alpha t} dt \quad (20)$$

The cyclic autocorrelation function presents the key descriptor of cyclostationary signals in two-dimensional time domain. When we reformulate the equation (20) by substitution (18) we obtained (Gardner, 1991)

$$\begin{aligned} R_{xx}^\alpha(\tau) &= \frac{1}{T} \int_{-\frac{T}{2}}^{\frac{T}{2}} x(t + \tau / 2) x^*(t - \tau / 2) e^{-i2\pi\alpha t} dt = \\ &= \frac{1}{T} \int_{-\frac{T}{2}}^{\frac{T}{2}} \left\langle \left[x(t + \tau / 2) e^{-i2\pi\alpha(t+\tau/2)} \right] \left[x(t - \tau / 2) e^{+i2\pi\alpha(t-\tau/2)} \right]^* \right\rangle dt = E\{u(t)v(t)\}. \end{aligned} \quad (21)$$

Now it is possible to bring out two others, but equivalent, definitions of cyclostationary signals (Gardner, 1991). Firstly, the signal $x(t)$ appears the second order periodicity ($x(t)$ is cyclostationary signal) if and only if the power spectral density of the delay-product signal (18) for some delays τ contains spectral lines at some nonzero frequencies $\alpha \neq 0$, that is if and only if $R_{xx}^\alpha(\tau) \neq 0$ is satisfied. Secondly, the multiplication with $e^{\pm i\pi\alpha t}$ shifts the signal $x(t)$ in the frequency domain of $\pm\alpha / 2$. The third definition of cyclostationarity is described in (Gardner, 1991); the cyclic autocorrelation function of a signal $x(t)$ is equivalent to cross-correlation function of the frequency shifted versions $u(t)$ and $v(t)$ of the same signal $x(t)$. The signal $x(t)$ exhibits second order cyclostationary if and only if the all vector of signal $x(t)$ is frequency shifted and correlated with each other vector; that is if $E\{u(t)v(t)\} = R_{xx}^\alpha(\tau)$ is not zero as a function of τ for some $\alpha \neq 0$.

Cyclic autocorrelation function is the descriptor in time domain. For many applications, it is more useful and convenient to apply the descriptor in frequency domain. The well-known is the Wiener-Khinchin theorem that determines the power spectral density by applying Fourier transform on autocorrelation function. When we apply the Fourier transform on the cyclic autocorrelation function, we obtain the so-called spectral correlation density function $S_x^\alpha(f)$ (SCDF), which represents the key descriptor of cyclostationary signals in frequency domain

$$S_x^\alpha(f) = F\{R_{xx}^\alpha(\tau)\} = \int_{-\infty}^{\infty} R_{xx}^\alpha(\tau) e^{-i2\pi f\tau} d\tau \quad (22)$$

It is convenient to use the form (23) for the real calculation of SCDF

$$S_x^\alpha(f) = \lim_{\Delta t \rightarrow \infty} \lim_{T \rightarrow \infty} \frac{1}{\Delta t} \frac{1}{T} \int_{-\Delta t/2}^{\Delta t/2} X_T(t, f + \frac{\alpha}{2}) X_T^*(t, f - \frac{\alpha}{2}) dt \quad (23)$$

where

$$X_T(t, f) = \int_{t-T/2}^{t+T/2} x(u) e^{-i2\pi fu} du, \quad (24)$$

is spectral component of $x(t)$ at frequency f with bandwidth $1/T$.

In the next sections, there will be shown simple application of cyclostationary descriptors on the tasks of symbol timing recovery and modulation recognition. In both cases the resistibility of this approach against additive white Gaussian noise will be investigated. The experiments were simulated in the MATLAB by partial usage the MATLAB code published in (Costa, 1996).

7. Symbol timing recovery experiment

The symbol timing recovery plays the critical role for reliable data detection in the digital communication receiver. In most cases the timing signal is derived from the demodulated signal received $x(t)$ (Barry et al, 2004). One of the methods used is based on spectral-line generation by applying nonlinear transformation. Because the timing signal usually has phase jitter, the phase lock loop (PLL) is used often to reduce it to the level desired. The general form of symbol timing recovery system based on spectral-line generation is shown in Fig. 6.

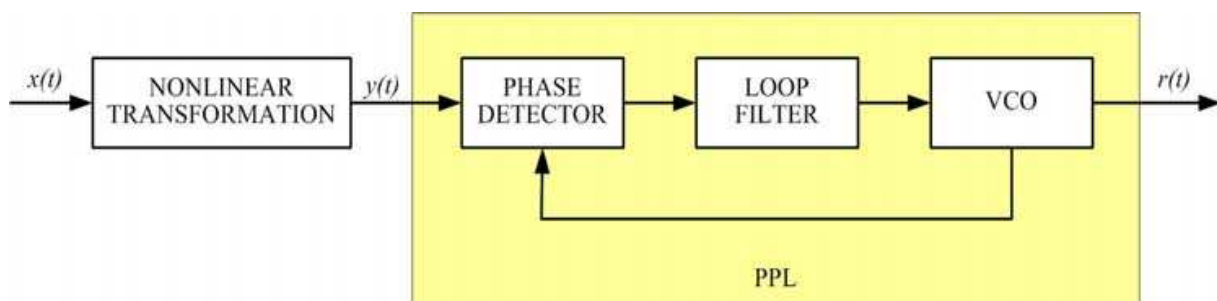


Fig. 6. General form of symbol timing recovery subsystem based on spectral line generation.

Some subsystems of symbol timing recovery exploit squaring of signal as nonlinear transformation. But squaring transformation works well only for certain types of data coding. For example, if signal $x(t)$ represents binary data with levels ± 1 , the square transform generates constant output signal $y(t) = x^2(t) = 1$ for all t (Gardner, 1991,1994). A more general is the quadratic transformation involving delays

$$y(t) = x(t)x(t - \tau) \quad (25)$$

where $x(t - \tau)$ is nonzero delay τ of signal $x(t)$. However, the relation (25) is equivalent to relation (18) for certain time lag τ . It is obvious that square transformation is a special case $y(t) = x(t+0)x^*(t-0) = x^2(t)$ of relation (18) too. So cyclic autocorrelation function is suitable for symbol timing recovery.

Next problem is to determine the optimal delay τ or by considering CAF optimal cyclic frequency α . It depends on particular modulation format as well as the pulse shape and data correlation. The mathematical derivations for some modulation types are described in (Gardner, 1986), (Lopez-Salcedo & Vazquez, 2003).

An experiment in the SIMULINK was simulated to show the timing recovery of BPSK modulated signal based on multiplication of demodulated signal and its delayed version (the delay equals to half of symbol period $\tau = T/2$). The schema of simulated system is shown in Fig. 7.

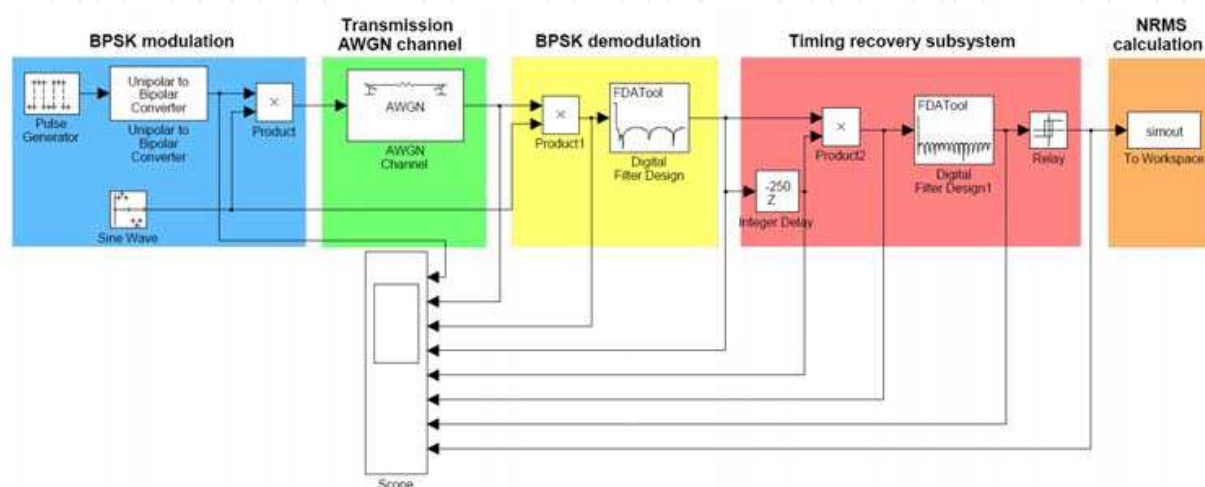


Fig. 7. The structure of simulated system in SIMULINK.

Appropriate timing behaviour of signals are displayed in Fig. 8.

Further, the simulation of timing recovery performance depending on AWGN in transmission channel was done. To the solution this problem, the ideal modulation data generated by the pulse generator (instead of random generator) were be used. The level of AWGN (E_b / N_0) in channel were adjusted from 50 to 5 dB. The difference of time position of rising edge of recovered timing signal and the ideal time position were be measured on the output $y(t)$. The method of normalized root mean square (RMS) of timing difference was been used as evaluation criteria. The results are shown in Fig. 9.

8. Modulation recognition experiment

The spectral correlation density function provides convenient classification criteria to be applied for modulation recognition. In contrast to traditional power spectral density function, which is often identical for different modulation type (example for BPSK, QPSK), SCDF can lead to different graphs (Gardner et all, 1987). Many works dealing with this problem were published (Gardner et all, 1987), (Qi et all, 2009). So, we try to simulate the SCDF of modulated signals BPSK and QPSK in MATLAB. Both signals were created with following parameters:

- sampling frequency 8192 Hz,
- carrier frequency 2048 Hz,
- symbol rate 512 b/s,
- data length 1024.

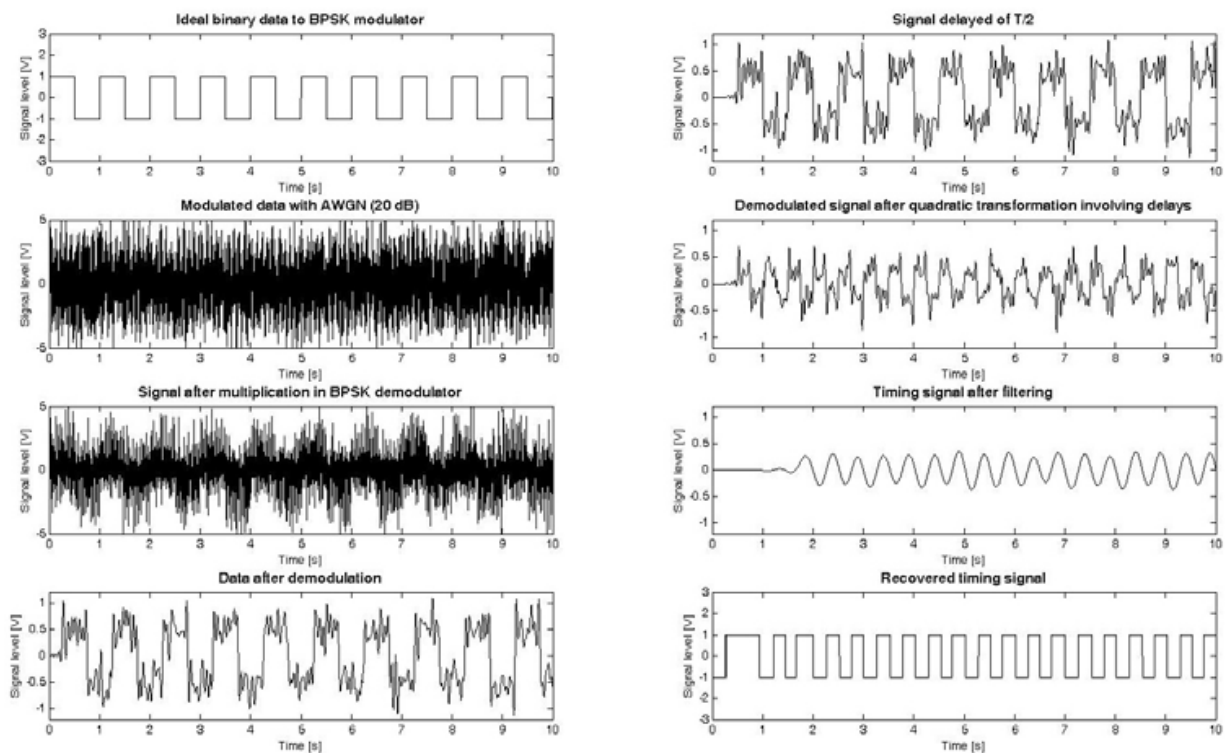


Fig. 8. Time behaviour of simulated signals.

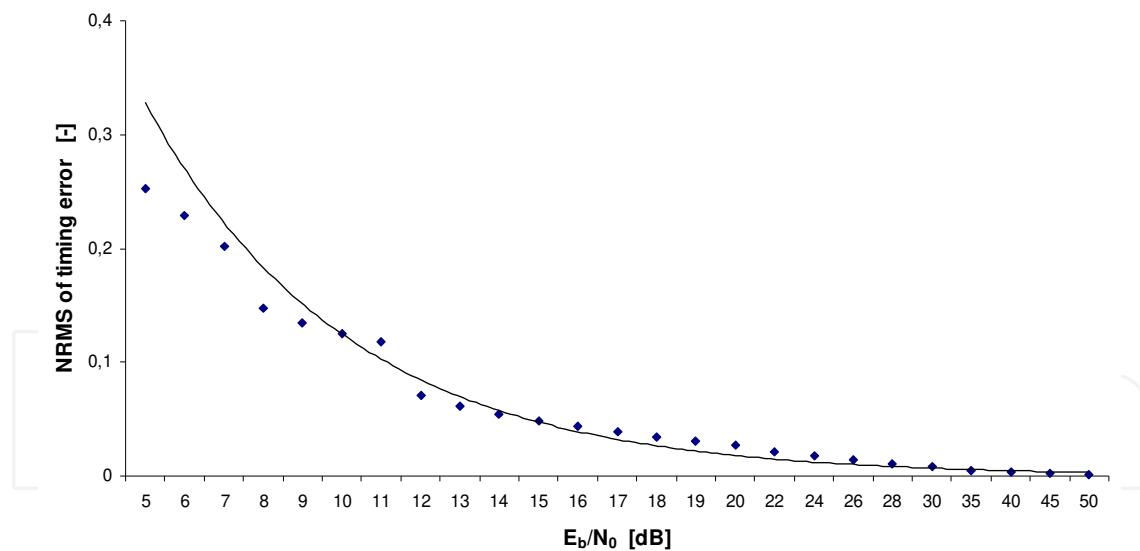


Fig. 9. Normalized RMS of timing error versus AWGN.

Obtained SCDF functions are shown in Fig. 10. Although PSK and QPSK signals have the same spectral density function, the graphic difference of both results (spectral correlation density functions of PSK and QPSK signal) is evident. We can split the graph to standard four quadrants and investigate the magnitude of maximum peak in each quadrant separately. While PSK signal has the equivalent level of magnitude for all peaks (quadrants), QPSK signal reaches in two opposed quadrants only about 50% of maximum. Exact value is dependant on statistical character of just utilized data and oscillates for each simulation.

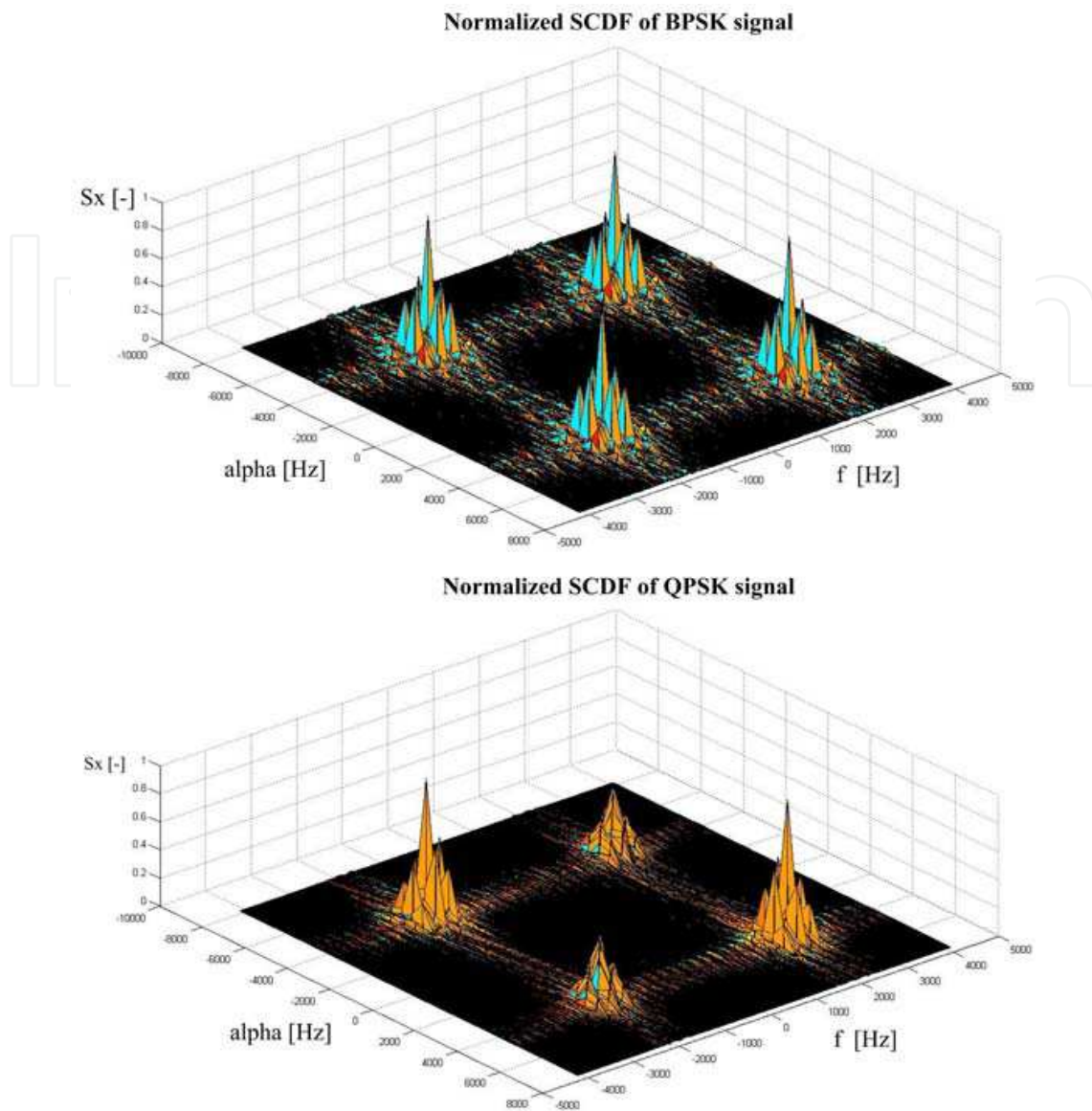


Fig. 10. Spectral Correlation Density Functions of PSK and QPSK signals

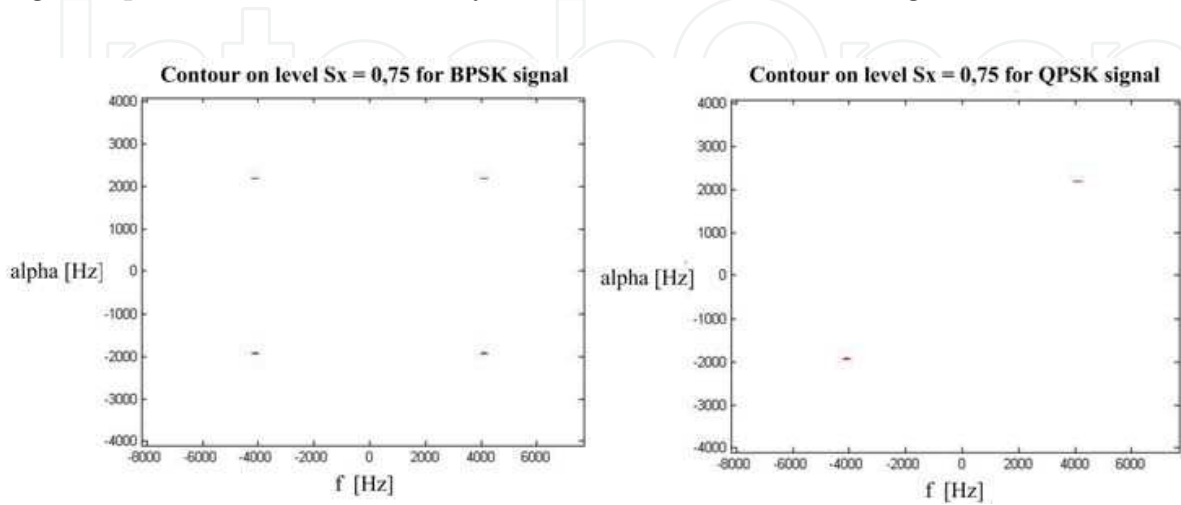


Fig. 11. Contours of normalized SCDF for modulation recognition

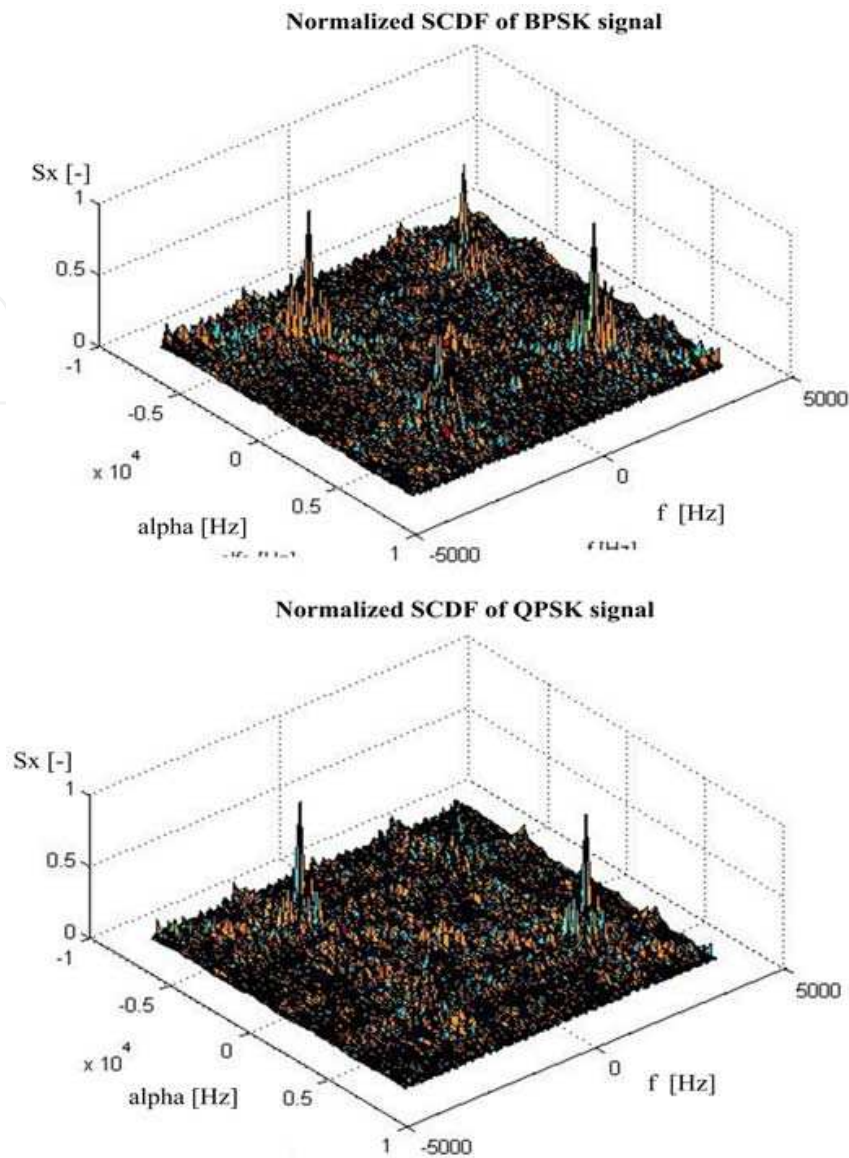


Fig. 12. Spectral Correlation Density Functions of PSK and QPSK signals for SNR = - 3 dB

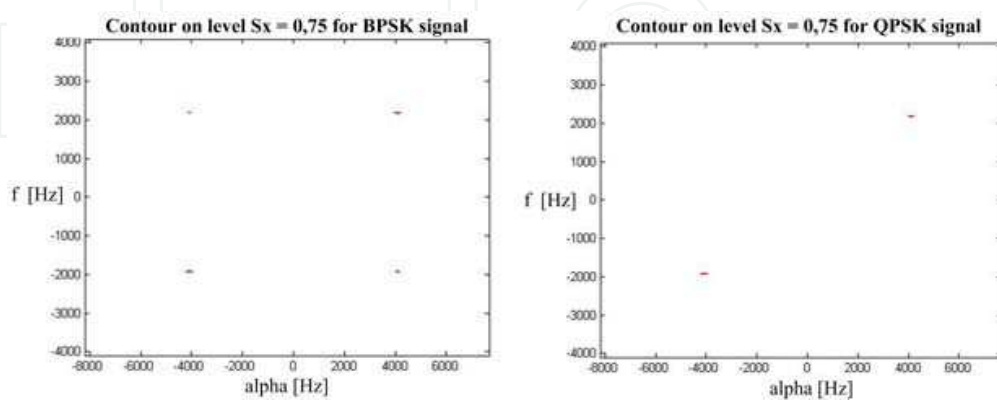


Fig. 13. Contours of normalized SCDF for modulation recognition for SNR = - 3 dB

Now we select very simply decision criteria for modulation recognition. If we make a contour of normalized SCDF on level 0,75 we obtain different results for each type modulation type.

For PSK signal it has four products while for QPSK signal it has only two products. The situation illustrate Fig. 11.

What can be more surprising is that this simply decision criteria works well under low level of signal to noise ratio (SNR). If we add to the signals additive white Gaussian noise it will work well. The results of simulation for SNR = - 3 dB are shown on Fig. 12 and Fig. 13.

9. Conclusion

The operation of the 2-class minimum-distance classifier of 2-FSK and 4-FSK signals has been verified by means of practical programming realized in the MATLAB programme. Results of the classification show that the Walsh-Hadamard transform has better properties for the recognition of FSK compared to Karhunen-Loeve transform (Richterova & Juracek, 2006). The classification efficiency of the 2-class minimum-distance classifier is superior to the linear classifier and quadratic classifier as presented in (Richterova, 2001). Experimental results show that the principal block scheme for the recognition of real pattern of 2-FSK and 4-FSK signals can be used for the special signal analysis in the areas where it is necessary to know or recognize the signal modulation type.

The experimental results indicate, that the 3-class minimum-distance classifier based on Karhunen-Loeve transform and the 3-class minimum-distance classifier based on Walsh-Hadamard transform are able recognize of three types of digital modulated signals. The number of correct classification for real patterns of FSK signals reaches approximately 70 %. The real patterns of PSK signals are classified correctly about 60 %. The designed classifiers are not able recognize modulation type 2-PSK and 4-PSK because the characteristic features of modulation type 2-PSK and 4-PSK are very similar. If we want recognize the groups of 2-PSK and 4-PSK, we must propose other type of modulation classifier.

The practical programming solution and performed experiments were verified a working 3-class minimum-distance classifier for the recognition of 2-FSK, 4-FSK and PSK signals. Results of the classification show that the Walsh-Hadamard transform has better properties for the recognition of FSK compared to Karhunen-Loeve transform. The results show, that this principle can be used for the technical analysis of signals in the branch, where necessary is obtained the information about the modulation type in the automatic system.

Although the theory of cyclostationary signals is known for several decades the practical research in this field still grows. New applications in cognitive radio (Sebesta, 2010), in military field (for example cyclostationary can be used to detect and identify ships, submarines or torpedoes in the ocean (Costa, 1996)) or in other scientific areas are investigated. This paper introduced the basic cyclostationary descriptors and on simply experiments demonstrates the effectiveness of this approach and its resistance against AWGN noise. The high resistance level results from correlation principle of cyclostationary method (useful signal) because mean value of AWGN correlation is zero.

There are many important aspects in cyclostationary measurement and application that were not mentioned here because of bounded length of paper. One of them is high sensitivity of obtained results on input parameters that is to say the input sequence length and required cyclic and frequency resolution. In some applications this leads on necessity of input signal pre-processing. The future research will be focus on automatic modulation recognition.

10. References

Ahmed, N.; Rao, K., R. (1975). *Orthogonal Transforms for Digital Signal Processing*. Springer-Verlag, Berlin, Germany.

- Barry, J. R.; Lee, E. A.; Messerschmitt, D. G. (2004). *Digital Communication*. (Third edition). Kluwer Academic Publishers, Dordrecht ISBN 0-7923-75483.
- Costa, E. L. (1996). *Detection and identification of cyclostationary signals*. (Ph.D. Thesis). Naval postgraduate school, Monterey, California.
- Gardner, W. A. The Role of Spectral Correlation in Design and Performance Analysis of Synchronizers. *IEEE Transactions on Communications*, vol. 34, no. 11., (November 1986), pp.1089-1095. ISSN 0090-6778.
- Gardner, W. A. *Exploitation of Spectral Redundancy in Cyclostationary Signals*. *IEEE Signal Processing Magazine*, vol. 8, no. 2, (April 1991), pp. 14-36, ISSN 1053-5888.
- Gardner, W. A. (1994) *Cyclostationarity in Communications and Signal Processing*. IEEE Press, New York, USA, ISBN 0-7803-1023-3.
- Gardner, W. A.; Brown, W.; Chin-Kang, C. Spectral Correlation of Modulated Signals: Part II-Digital Modulation. *IEEE Transactions on Communications*, vol. 35, no. 6, (June 1987), pp. 595-601, ISSN 0096-2244.
- Gardner, W.; Napolitano, A.; Paura, L. Cyclostationarity: Half a century of research. *Signal processing*, vol. 86, no. 4, (2006), pp. 639-697, ISSN 0165-1684.
- Grimaldi, D.; Rapuano, S.; De Vito, L. An Automatic Digital Modulation Classifier for Measurement on Telecommunication Networks. *IEEE Transactions on Instrumentation and Measurement*, vol. 56, no. 5, (2007), pp. 1711-1720.
- Hua, Y.; Liu, W. Generalized Karhunen-Loeve transform. *IEEE on Signal Processing Letters*, vol. 5, no. 6, (1998), pp. 141-142.
- Jondral, F. (1991). *Funksignalanalyse*. Teubner, Stuttgart, Germany.
- Lopez-Salcedo, J., A.; Vazquez, G. Stochastic Approach to Square Timing Estimation with Frequency Uncertainty. *Proceedings of IEEE International Conference on Communications (ICC'03)*, vol. 5, pp. 3555-3559, ISBN 0-7803-7802-4, Anchorage, AK, May 2003.
- Nandi, A, K.; Azzouz, E.E. Algorithms for Automatic Modulation Recognition of Communication Signals. *IEEE Transactions on Communications*, vol. 46, no. 4., (1998), pp. 431 - 436.
- Park, Ch.-S.; Dae, Y., K. A Novel Robust Feature of Modulation Classification for Reconfigurable Software Radio. *IEEE Transactions on Consumer Electronics*, vol. 52, no. 4, (2006), pp. 1193-1200.
- Qi, Y., Peng, T., Wang, W., Luo, S. Cyclostationary signature design for common control channel of cognitive radio. *The Journal of China Universities of Posts and Telecommunications*, vol. 16, no. 2, (April 2009), pp. 42-46, ISSN 1005-8885.
- Richterova, M.; Juracek, D. Modulation classifiers based on orthogonal transforms. *Proceedings of the ITTE International Conference "C2 Systems and NATO NEC"*, pp. 14-18, University of Defence, Brno, Czech Republic, May 10-11, 2006.
- Richterova, M. (2001) *Contribution to recognition of data modulated signals (in Czech)*. (PhD Thesis). Military Academy, Brno, Czech Republic, 2001.
- Richterova, M. A 2-class classifier of FSK signals. signals (in Czech), *Proceedings of STO-6*, pp. 22-27, Military Academy, Brno, Czech Republic, September 22-23, 1997.
- Richterova, M. Modulation Recognition in Radiocommunication Systems. *Proceedings of A XXVIII. Sesiune de Comunicari Stiintifice cu Participare Internationala*, pp.36-42, ATM, Bucharest, Romania, October 1999.
- Semmlow, J. L. (2004) *Biosignal and Biomedical Image Processing. MATLAB-Based Applications*. CRC Press, New York, USA, ISBN 0-8247-4803-4.
- Sebesta, V. Estimating a Spectral Correlation Function under the Conditions of Imperfect Relation between Signal Frequencies and a Sampling Frequency. *Radioengineering*, vol. 19, no. 1, (2010), ISSN 1210-2512.



Applications of MATLAB in Science and Engineering

Edited by Prof. Tadeusz Michalowski

ISBN 978-953-307-708-6

Hard cover, 510 pages

Publisher InTech

Published online 09, September, 2011

Published in print edition September, 2011

The book consists of 24 chapters illustrating a wide range of areas where MATLAB tools are applied. These areas include mathematics, physics, chemistry and chemical engineering, mechanical engineering, biological (molecular biology) and medical sciences, communication and control systems, digital signal, image and video processing, system modeling and simulation. Many interesting problems have been included throughout the book, and its contents will be beneficial for students and professionals in wide areas of interest.

How to reference

In order to correctly reference this scholarly work, feel free to copy and paste the following:

Richterova Marie and Mazalek Antonin (2011). Classifiers of Digital Modulation Based on the Algorithm of Fast Walsh-Hadamard Transform and Karhunen-Loeve Transform, Applications of MATLAB in Science and Engineering, Prof. Tadeusz Michalowski (Ed.), ISBN: 978-953-307-708-6, InTech, Available from: <http://www.intechopen.com/books/applications-of-matlab-in-science-and-engineering/classifiers-of-digital-modulation-based-on-the-algorithm-of-fast-walsh-hadamard-transform-and-karhun>

INTECH
open science | open minds

InTech Europe

University Campus STeP Ri
Slavka Krautzeka 83/A
51000 Rijeka, Croatia
Phone: +385 (51) 770 447
Fax: +385 (51) 686 166
www.intechopen.com

InTech China

Unit 405, Office Block, Hotel Equatorial Shanghai
No.65, Yan An Road (West), Shanghai, 200040, China
中国上海市延安西路65号上海国际贵都大饭店办公楼405单元
Phone: +86-21-62489820
Fax: +86-21-62489821

© 2011 The Author(s). Licensee IntechOpen. This chapter is distributed under the terms of the [Creative Commons Attribution-NonCommercial-ShareAlike-3.0 License](#), which permits use, distribution and reproduction for non-commercial purposes, provided the original is properly cited and derivative works building on this content are distributed under the same license.

IntechOpen

IntechOpen